Universidad Industrial de Santander

Synthesis and optimization of properties of thin films of FAx(MA1-X)PbI3 grown by spin coating with perovskite structure to be used as active layer in hybrid solar cells

Síntesis y optimización de propiedades de películas delgadas de FAx(MA1-X)PbI3 crecidas por spin coating con estructura perovskita para ser usadas como capa activa en celdas solares híbridas

Gerardo Gordillo-Guzmán[1a], Ophyr Virgüez-Amaya[2], Camilo Otálora-Bastidas[3], Clara Calderón-Triana[1b], César Quiñones-Segura[4]

[1]Departamento de Física, Universidad Nacional de Colombia, Bogotá, Colombia.
Orcid: [a] 0000-0002-1239-8103, [b] 0000-0002-3149-2939. Emails: [a] ggordillog@unal.edu.co,
[b] clcalderont@unal.edu.co
[2] Fundación Universidad de América, Bogotá, Colombia. Orcid: 0000-0002-7676-4926.
Email: ophyr.virguez@estudiantes.uamerica.edu.co
[3]Escuela de Ingenierías Eléctrica, Electrónica y de Telecomunicaciones, Universidad Industrial de Santander,
Santander, Colombia. Orcid: 0000-0002-5330-0408. Email: camilo.otalora@correo.uis.edu.co
[4]Institución Universitaria Politécnico Grancolombiano, Bogotá, Colombia. Orcid: 0000-0002-5001-1627.
Email: profecesarq@gmail.com

Abstract

This work reports results concerning the effect that the substitution of the methylammonium cation by the formamidinium cation causes on the properties of $FA_x(MA_{1-x})PbI_3$ films synthesized by spin coating in one step. For that, it was conducted a study to establish the influence of the composition of the $FAx(MA_{1-x})PbI_3$ films on their optical, structural and morphological properties, determined through spectral transmittance, atomic force microscopy, and x-ray diffraction measurements. Correlating parameters of synthesis with results of the study of properties performed, it was able to get conditions to grow $FA_x(MA_{1-x})PbI_3$ films with an improved optical gap, microstructure and morphology, what allows to think that this compound is suitable to be used as the active layer in hybrid solar cells.

Keywords: chemical composition; methylammonium cation; formamidinium cation; antisolvent treatment.

Resumen

Este trabajo reporta resultados relacionados con el efecto que la sustitución del catión methylammonium por el catión formamidinium causa sobre las propiedades de las películas de $FA_x(MA_{1-x})PbI_3$ sintetizadas por spin coating en un paso. Para esto se realizó un estudio que estableciera la influencia de la composición de las películas de

$FA_x(MA_{1-x})PbI_3$ sobre sus propiedades ópticas, estructurales y morfológicas, determinadas a través de medidas de transmitancia espectral, microscopía de fuerza atómica y difracción de rayos-X. Correlacionando parámetros de síntesis con los resultados del estudio de propiedades realizado, fue posible obtener las condiciones para crecer películas de $FA_x(MA_{1-x})PbI_3$ con gap óptico mejorado, microestructura y morfología, que permite pensar que este compuesto es adecuado para ser usado como capa activa en celdas solares híbridas.

Palabras clave: composición química; catión methylammonium; catión formamidinium; tratamiento antisolvente.

1. Introduction

Despite the few years of development of Perovskite based solar cells, huge progress has been made [1-5], achieving in a short time efficiencies greater than 22% [6]. The hybrid organic/inorganic perovskite materials have a generic structure ABX_3, where A is a monovalent cation (usually methylammonium (MA) $CH_3NH_3^+$, formamidinium (FA) $CH_3(NH_2)_2^+$), B is a divalent metal (Pb^{2+} or Sn^{2+}) and an anion X (Cl^- ; Br^- ; I^-). Perovskite thin films can be processed using various techniques including spin coating [7], dip coating [8] and evaporation in vacuum ambient [9] making them one of the most versatile photovoltaic (PV) technologies.

High Perovskite solar cells performances have been attributed to exceptional material properties and a tunable band gap from 1.1 to 2.3 eV [10]. However, there are concerns with respect to the degradation of the ABX_3 compounds upon contact with moisture as well as light-induced trap-state formation [11]. In particular, the compound $MAPbI_3$ (MAPI) tends to degrade when it is exposed to a humid environment and the compound $FAPbI_3$ (FAPI) is structurally unstable at room temperature and grows in a non-photoactive phase (hexagonal δ-$FAPbI_3$); however, this compound recrystallizes in the ideal phase α-$FAPbI_3$ (photoactive) at high temperatures [12 ,13].

This work reports results related to the effect that the incorporation of formamidinium in the structure of thin films of $CH_3NH_3PbI_3$ (MAPbI_3) deposited by spin coating has on its stability as well as on the morphological, structural and optical properties.

2. Methodology

$Cs_xFA_{1-x}PbI_3$ thin films were deposited in one step by spin-coating at 4000 rpm, using a solution 1M with composition $MA_xFA_{1-x}PbI_3$ ($0<x<1$) in γ-Butyrolactone
(GBL), followed by antisolvent treatment consisting of the addition of a second solvent maintaining the sample in rotation and then annealed for 10 minutes at 110^0 C. The antisolvent treatment was carried out using toluene, dichloromethane and ethyl acetate as second solvent,

which were added during time intervals that varied between 5 and 40 seconds.

The solution used for the synthesis of $MA_xFA_{1-x}PbI_3$ films was prepared mixing lead iodide (PbI_2) with a mixture of metilamonium iodide (MAI) and formamidinium iodide (FAI). The PbI_2 used are commercial reagent (Sigma Aldrich) while the FAI and MAI precursors were synthesized in our laboratory following the procedure described in Ref [14].

The $MA_xFA_{1-x}PbI_3$ samples were characterized by means of diffuse reflectance measurements performed using a Varian Cary 5000 spectrophotometer, as well as by X-ray diffraction (XRD) measurements performed with a Philips X'Pert Pro PANalytical diffractometer, using the radiation Cu-Kα (1.540598 Å), an acceleration voltage of 40 KV and a current 40 mA; the atomic force microscopy (AFM) images were done with a PSI Auto-probe CP microscope in contact mode and the film thickness was determined using a Veeco Dektak 150 surface profiler.

3. Results and discussion

3.1. Identification of the phases present in the $FA_xMA_{1-x}PbI_3$ films

The phases present in thin $FA_xMA_{1-x}PbI_3$ films prepared with different FA/MA ratios ($0 \leq x \leq 1$) and subjected to antisolvent treatment, were identified by means of XRD measurements. In Figure 1 are shown XRD spectra of $FA_xMA_{1-x}PbI_3$ films prepared varying the FA/MA ratio from x=0 to x=1.0. It is observed $MAPbI_3$ samples (x=0) exhibit diffraction peaks at 2θ=14.14°, 20.02°, 24.51, 28.47° 31.89°, 33.7°, 40.61° and 43.15° corresponding to the reflection planes (110), (112), (211), (202), (220), (310), (224) and (330) that have been assigned to the black phase of perovskite with tetragonal crystalline structure (space group I4/mcm, a=8,896 Å, c=12,698 Å) [15,16]. The samples prepared with composition corresponding to $0.2 \leq x \leq 0.6$ present an additional reflection at 2θ=13.9^0 which has been assigned to the α-$FAPbI_3$ phase [17], indicating that this type of samples grows with a mixture of the phases $MAPbI_3$ and α-$FAPbI_3$. It is also observed that samples prepared with composition corresponding to x$\geq$0.8

Synthesis and optimization of properties of thin films of $FA_x(MA_{1-X})PbI_3$ grown by spin coating with perovskite structure to be used as active layer in hybrid solar cells

REVISTA UIS INGENIERÍAS 89

present new reflections that have been assigned to the PbI_2 phase and to the yellow phase δ-FAPbI$_3$ [18]. Theinset of figure 1 are shown scans of the diffractograms around the peak at $2\theta=14.14°$.
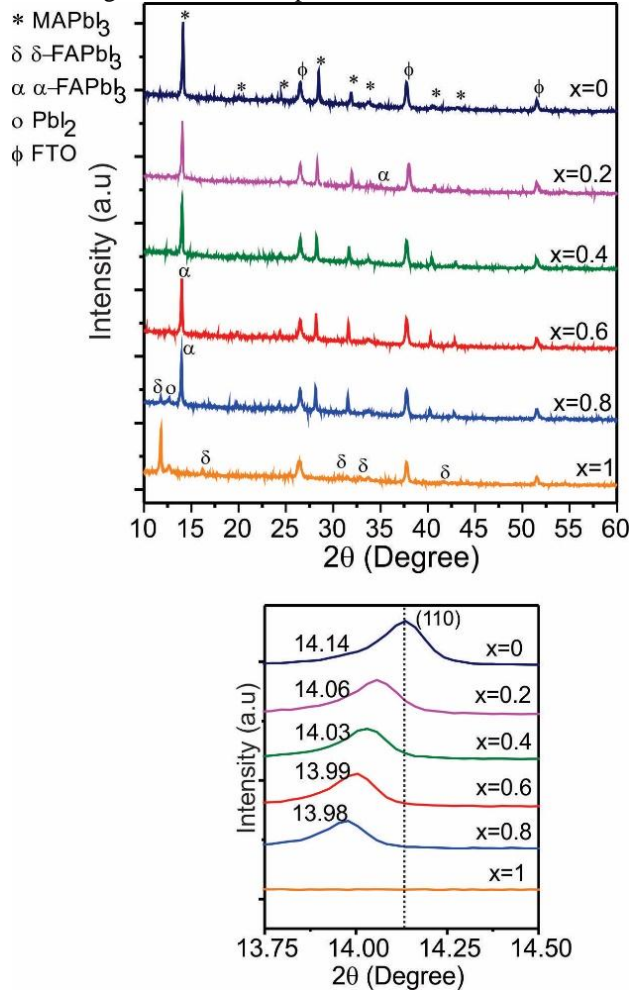

Figure 1. Difractograms obtained for $FA_xMA_{1-x}PbI_3$ films with different FA/MA ratio. Inset below shows scans of the diffractograms around the peak at $2\theta=14.14°$. Source: own elaboration.

3.2 Study of degradation of $FA_xMA_{1-x}PbI_3$ films

The effect that the incorporation of FA on the structure of MAPbI$_3$ films has on the stability of the $FA_xMA_{1-x}PbI_3$ films, was evaluated through measurements of XRD made after its deposition and after several days of being exposed to the environment. In figure 2 are displayed XRD spectra of typical MAPI, FAPI, and $FA_{0.4}MA_{0.6}PbI_3$ films, measured after being exposed to the environment for several days. A sweep was made between $2\theta=10^0$ and $2\theta=15^0$ considering that peaks

associated with secondary phases appear in this region, as a result of the degradation of the samples.
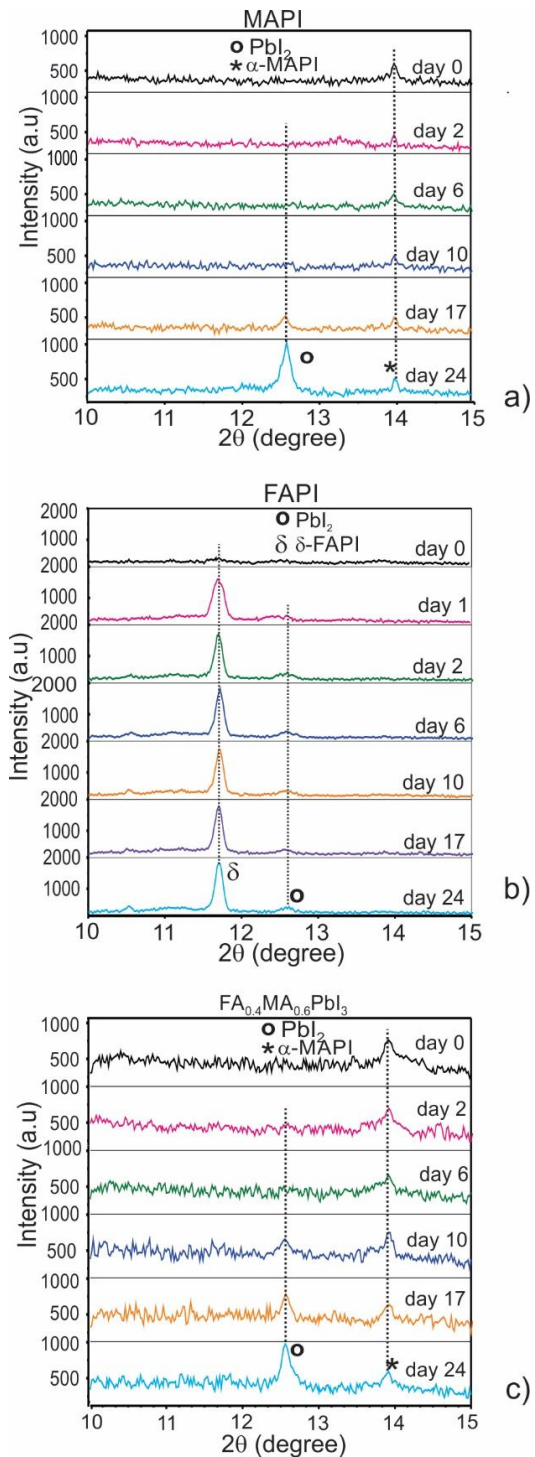

Figure 2. XRD spectra of thin films of a) MAPbI$_3$ b) FAPbI$_3$ and c) $FA_{0.4}MA_{0.6}PbI_3$, measured after its preparation and after 1 to 24 days of being exposed to the environment. Source: own elaboration.

Figure 2 illustrates that in samples of MAPI, the peak at $2\theta=12.6^0$ which is characteristic of the PbI_2 phase, appears after 15 days; in samples of FAPI two peaks in $2\theta=12.6$ and $2\theta=11.7$ associated to the PbI_2 and δ-$FAPbI_3$ phases appears a few hours after the deposition. These results indicate that both MAPI and FAPI samples are degraded when exposed to the environment, with FAPI films being much more unstable than those of MAPI. On the other hand, it is observed that in samples of $FA_{0.4}MA_{0.6}$ PbI_3, the peak associated with the PbI_2 phase appears after 6 days of exposure to the environment, indicating that this type of sample is more stable than those of FAPI but less stable than the MAPI samples. The better stability against moisture exposure of MAPI is related to the fact that MAPI has a better tolerance factor (TF=9.0) than FAPI (TF=10) [19], associated with the greater ionic radius of the FA.

The main degradation mechanism of MAPI and FAPI compounds when were exposed to moisture and oxygen from the environment, has been attributed to a catalytic reduction of these compounds in PbI_2, CH_3NH_2 (or $CH_3(NH)_2$) and HI [20].

In contrast to $MAPbI_3$, which, upon exposure to humidity, decomposes to PbI_2 and volatile organic phases, FA-based perovskite exhibits a change in color from dark to yellow due to an undesirable phase transition from the α to δ-phase [21]. This transition is highly undesirable for photovoltaic applications, since the non-perovskite δ-phase has a significantly larger bandgap and inferior charge-transport properties.

3.3 Effect of incorporating the cation FA in the structure of MAPbI₃ films on the microstructure of FAₓMA₁₋ₓPbI₃ films

It has found the full width at half maximum (FWHM) value of $FA_xMA_{1-x}PbI_3$ films is affected by the amount of MA cations substituted by FA cations, indicating that this parameter affects its crystallinity. On the other hand, considering that the peak broadening is affected by crystallite size D and lattice strain $\mathcal{E}$ (relative change in size with respect to the size before experiencing an external force) induced by structural defects [22], these two parameters were determined by the X-ray line broadening method using the Williamson-Hall equations [23] given by:

$$\beta_{hkl}cos\theta_{hkl} = \frac{K\lambda}{D} + 4\varepsilon sin\theta_{hkl} \qquad (1)$$

where D is the crystallite size, λ is the wavelength of the CuKα radiation, k is a constant equal to 0.94, β_{hkl} is the

peak width at a half-maximum intensity and θ_{hkl} is the peak position.

Plotting the term $\beta cos\theta$ with respect to $4sin\theta$ for the preferred orientation peaks, the strain and crystallite size can be obtained from the slope and y-intersect of the fitted line. The values of D and $\mathcal{E}$ estimated from the UDM model are summarized in Table 1.

The results of table 1 show that an increase in the proportion of ions of MA that are replaced by ions of FA, gives rise to a slight increase of the crystallite size of the $FA_xMA_{1-x}PbI_3$ films; these results also show that the lower values of microstrain $\mathcal{E}$ are obtained by replacing the ion MA with the ion FA in proportions between 40% and 60%, indicating that the substitution of MA by FA in the above-mentioned proportions results in the growth of $FAMAPbI_3$ samples with improved crystallinity.

Table 1. Influence of the FA:MA ratio on the crystallite size D and micro-strain $\mathcal{E}$ of $FA_xMA_{1-x}PbI_3$ films.

Composition	Crystallite size		Strain
X	Scherrer (nm)	W-H (nm)	$\mathcal{E}$ x10⁻⁴
0	58.05	60.21	5.1
0.2	57.94	60.72	4.6
0.4	59.36	62.02	3.9
0.6	59.05	62.80	4.3
0.8	62.97	63.02	4.9
1.0	65.27	69.32	8.4

Source: own elaboration.

3.4 Effect of incorporating the cation FA in the structure of MAPbI₃ films on the optical properties of FAₓMA₁₋ₓPbI₃ films

The effect of the amount of FA incorporated in the structure of $MAPbI_3$ films on the optical gap of $FA_xMA_{1-x}PbI_3$ films was evaluated through diffuse reflectance measurements. For this, it used a method described by A. B. Morphy based on the Kubelka, Munk theory [24], which allows determining the absorption coefficient (α) and energy band gap (Eg) of materials thatscatter light, from measurements of diffuse reflectance [25]. Initially, the absorption coefficient is calculated from diffuse reflectance measurements and then, taking the values of α found and considering that for direct gap materials the relationship $(F(R)hv)^2 = A (hv-Eg)$ is fulfilled, the value of Eg can be determined from the intercept with the hv axis that results from

Synthesis and optimization of properties of thin films of $FA_x(MA_{1-X})PbI_3$ grown by spin coating with perovskite structure to be used as active layer in hybrid solar cells

REVISTA UIS INGENIERÍAS 91

extrapolating the linear region of the curve $(F(R)hv)^2$ vs hv. In figure 3 are displayed curves of diffuse reflectance and $(F(R)hv)^2$ vs hv obtained for $FA_xMA_{1-x}PbI_3$ films, prepared varying the FA content between x=0 and x=1.0.
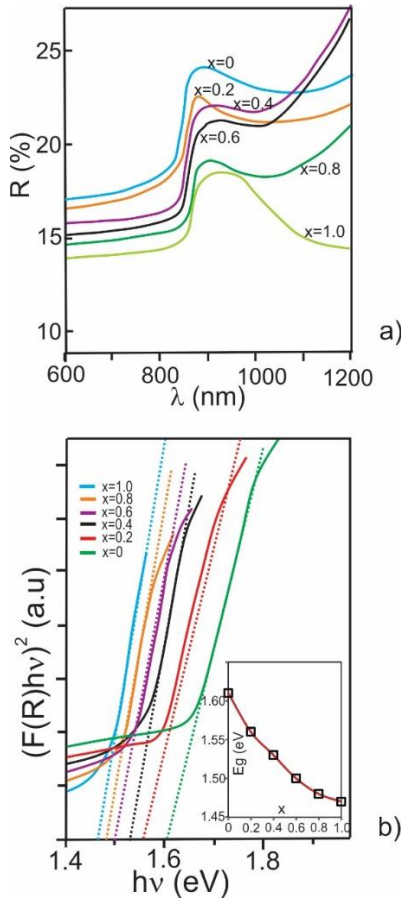

Figure 3. Curves of diffuse reflectance and $(F(R)hv)^2$ vs hv, corresponding to $FA_xMA_{1-x}PbI_3$ films prepared varying the FA content between x=0 and x=1.0. Source: own elaboration.

As shown in figure 3, an increase in the proportion FA:MA gives rise to an Eg decrease, from a value of 1.61 eV for the sample of composition $MAPbI_3$ until a value of 1.47 eV for the sample of composition $FAPbI_3$, indicating that the incorporation of FA in the structure of the $FAPbI_3$ leads to a change in the structure of bands, apparently induced by the expansion produced in the lattice of the $FA_xMA_{1-x}PbI_3$ as a consequence of the larger size of the ion FA compared with that of the ion MA. These results agree with those reported by other authors [26], who also observed a decrease in the value of Eg by increasing the proportion FA:MA.

It is well known that the presence of structural defects generates states of tails of bands that participate in photons absorption processes which can be evaluated through the calculation of the absorption coefficient near the band edge (α_U) that has an exponential dependence on photon energy and Urbach energy [26] given by:

$$\alpha_U = \alpha_0 exp \left[\frac{hv - E_i}{Eu} \right] \tag{2}$$

Where E_u is the Urbach energy, E_i and α_0 are constant. Thus, a plot of $ln\alpha$ vs hv should be linear and Urbach energy can be obtained from the slope. In Table 2 are the values of the Urbach energy of $FA_xMA_{1-x}PbI_3$ films, prepared varying the FA:MA ratio.

Table 2. Influence of the FA:MA ratio on the Urbach energy of $FA_xMA_{1-x}PbI_3$ films.

x	0	0.2	0.4	0.6	0.8	1.0
E_u(meV)	139	134	108	87	79	68

Source: own elaboration.

Table 2 reveals that the value of Eu decreases by increasing the FA:MA ratio, indicating that an increase in the amount of FA incorporated in the structure of the compound $MAPbI_3$ yields an increase of the structural defects.

Recently Yang Li et al. made a publication [27] in which they emphasize systematically describing the methodologies for manufacturing Perovskite materials based on FA that have been more successful, such as additive engineering, intermolecular exchange, interfacial engineering in solution processing, and chemical vapor deposition and presented a detailed discussion of the relationship between fabrication methods, film properties, and device efficiency. In particular, this paper reported the band gap value of $FAPbI_3$ films prepared by different methods varies between 1.40 and 1.47 eV, which agrees with the one obtained in this work. In addition, we have found that the FA-perovskite has a narrower bandgap compared with pure $MAPbI_3$, a result that also agrees with that reported by Yang Li et al.

The main difference between the results obtained from this work and those reported in the paper by Yang Li et al., is about this report put special emphasis on the effect that the substitution of the MA cation with the FA cation causes on the properties of $FA_x (MA_{1-x}) PbI_3$

films synthesized by spin coating, while in the paper by Yang Li et al., it focuses on making a discussion of the effect that the synthesis method of FAPbI$_3$ films creates on the film properties and device efficiency.

3.5 Effect of FA incorporation in the MAPbI$_3$ structure on the morphology of FA$_x$MA$_{1-x}$PbI$_3$ thin films

The effect of incorporating FA in the MAPbI$_3$ structure on the FA$_x$MA$_{1-x}$PbI$_3$ morphology films prepared with different FA:MA ratios and subjected to antisolvent treatment with toluene, was studied through AFM measurements. Figure 4 shows AFM images of typical FA$_x$MA$_{1-x}$PbI$_3$ thin films prepared with different FA/MA ratios and the grain size of the samples is shown in Table 3. These results reveal in general, the FA$_x$MA$_{1-x}$PbI$_3$ films grow with a sub-micrometric size compact grains structure and that their grain size increases by increasing the FA:MA ratio.
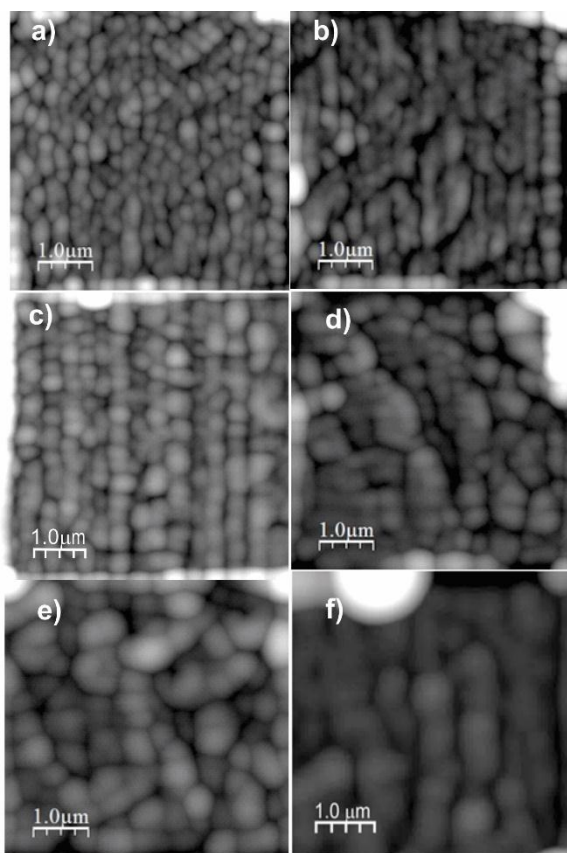

Figure 4. AFM images of typical FA$_x$MA$_{1-x}$PbI$_3$ films submitted to antisolvent treatment with toluene, with compositions corresponding to a) x=0, b) x=0.2, c) x=0.4, d) x=0.6, e) x=0.8 and f) x=1.0. Source: own elaboration.

Table 3. Grain size of the FA$_x$MA$_{1-x}$PbI$_3$ films obtained from the AFM images.

x	Grain size (nm)
0	221.37
0.2	245.95
0.4	310.50
0.6	380.05
0.8	396.85
1	438.50

Source: own elaboration.

4. Conclusions

The effect that the substitution of the ion MA by the ion FA causes on the optical, structural and morphological properties of FA$_x$MA$_{1-x}$PbI$_3$ films prepared by spin coating in one step, was studied through diffuse reflectance, AFM and XRD measurements. From these studies, it was found that the samples with composition MAPbI$_3$ (x=0) grow in the CH$_3$(NH$_2$)$_2$PbI$_3$ phase with tetragonal perovskite-type structure, whereas the samples prepared replacing the ion MA by the ion FA in a proportion less than 20% grow with a mixture of the tetragonal MAPbI$_3$ and the *-FAPbI$_3$ phases. When the substitution is greater than 80%, the samples grow with a mixture of the PbI$_2$ phase and the yellow phase δ-FAPbI$_3$. Evaluation of the degradation through XRD measurements made after the deposition and after several days of exposure to the environment, indicated that samples with a composition corresponding to x=0 (MAPI) are significantly more stable than samples whom the MA cation is replaced by the FA cation. In particular, thin films of FAPI (x=1) initiate their degradation only a few hours after being deposited.

Estimation of the <u>microstrain</u> $\mathcal{E}$ value of FA$_x$MA$_{1-x}$PbI$_3$ films, made through XRD measurements, indicated that in general samples prepared with composition x between 0.4 and 0.6 grew with improved crystallinity. It was also found that an increase in the proportion FA:MA gives rise to a *Eg decrease*, from a value of 1.61 eV for samples of composition MAPbI$_3$ (x=0) until a value of 1.47 eV for samples with composition x=1 (FAPbI$_3$).

AFM measurements revealed that the morphology of FA$_x$MA$_{1-x}$PbI$_3$ thin filmsis significantly improved through anti-solvent treatment. These samples exhibited in general formation of compact grains that resulted in a good degree of substrate coverage. This study also revealed that an increase of the FA:MA proportion gives rise to an increase in the grain size.

Synthesis and optimization of properties of thin films of $FA_x(MA_{1-X})PbI_3$ grown by spin coating with perovskite structure to be used as active layer in hybrid solar cells

REVISTA UIS INGENIERÍAS 93

Acknowledgements

References

[1] L. Mingzhen, M.B. Johnston, H.J. Snaith. "Efficient planar heterojunction perovskite solar cells by vapour deposition", *Nature*, vol. 501, no. 7467, pp. 395-398, 2013. doi: 10.1038/nature12509.

[2] N.G. Park. "Organometal perovskite light absorbers toward a 20% efficiency low-cost solid-state mesoscopic solar cell", *Journ. Phys Chem Lett,* vol. 4, pp. 2423-2429, 2013. doi: 10.1021/jz400892a.

[3] S. Kazim *et al.*, "Perovskite as light harvester: A game changer in photovoltaics", *Angew Chem Int Ed Engl,* vol. 53 pp. 2812-2824, 2014. doi: 10.1002/anie.201308719.

[4] J.H. Heo *et al.*, "Hysteresis-less inverted $CH_3NH_3PbI_3$ planar perovskite hybrid solar cells with 18.1% power conversion efficiency", *Energ Environ Sci,* vol. 8, no. 5, pp. 1602-1608, 2015. doi: 10.1039/c5ee00120j.

[5] C. Chien-Hung, W. Chun-Guey, "Bulk heterojunction perovskite: PCBM solar cells with high fill factor", *Nature Photonics*, vol. 10, no.3, pp. 196-200, 2016. doi: 10.1038/nphoton.2016.3.

[6] The National Renewable Energy Laboratory, "Best Research-Cell Efficiency Chart Photovoltaic Research," *NREL*, 2018. [online] Available: https://www.nrel.gov/pv/cell-efficiency.html.

[7] M.M. Lee *et al.,* "Efficient hybrid solar cells based on meso-superstructured, organometal Halide perovskites", *Science*, vol. 338, pp. 643-647, 2012. doi: 10.1126/science.1228604

[8] J. Burschka *et al.*, "Sequential deposition as a route to high-performance perovskite-sensitized solar cells", *Nature*, vol. 499, pp. 316-319, 2013. doi: 10.1038/nature12340.

[9] O. Malinkiewicz *et al.*, "Perovskite solar cells employing organic charge-transport layers", *Nature Photonics*, vol. 8, pp. 128-132, 2014. doi: 10.1038/nphoton.2013.341.

[10] S.D. Stranks *et al.*, "Electron-hole diffusion lengths exceeding 1 micrometer in an organometal Trihalide perovskite absorber", *Science,* vol. 342, no. 6156, pp. 341-344, 2013. doi: 10.1126/science.1243982.

[11] B. Conings *et al.*, "Intrinsic thermal instability of Methylammonium Lead Trihalide perovskite", *Adv. Energy Mater*, vol. 5, no. 15, pp. 1-8, 2015. doi: 10.1002/aenm.201500477.

[12] W. Xie, Y. Wang, X. Zhang, "Synthesizing conditions for organic-inorganic hybrid perovskite using methylammonium lead iodide", *Journ. of Phys and Chem of Solids*, vol. 105, pp. 16-22, 2017. doi: 10.1016/j.jpcs.2017.02.002.

[13] The National Renewable Energy Laboratory, "Explanatory Notes for NREL's 'Best Research-Cell Efficiencies' Chart.", [online] Available: https://www.nrel.gov/pv/assets/pdfs/cell_efficiency_exp lanatory_notes.pdf

[14] G. Gordillo, C.A. Otálora, M.A. Reinoso, "Trap center study in hybrid organic-inorganic perovskite using thermally stimulated current (TSC) analysis", *Journ. Appl. Phys,* vol. 122, no. 075304, 2017. doi: 10.1063/1.4999297.

[15] A. Ghada *et al.*, "Effect of temperature on light induced degradation in methylammonium lead iodide perovskite thin films and solar cells", *Sol. Energy Mater. Sol. Cells* vol. 174, pp. 566-571, 2018. doi: 10.1016/j.solmat.2017.09.053.

[16] S. Xu-Guang *et al.*, "Effect of CH_3NH_3I concentration on the physical properties of solution-processed organometal halide perovskite $CH_3NH_3PbI_3$", *Journ. of Alloys and Compounds*, vol. 706, pp. 274-279, 2017. doi: 10.1016/j.jallcom.2017.02.256.

[17] Z. Yi *et al.*, "Optimization of stable quasi-cubic; $FA_xMA_{1-x}PbI_3$ perovskite structure for solar cells with efficiency beyond 20%", *ACS Energy Lett*, vol. 2, pp. 802-806, 2017. doi: 10.1021/acsenergylett.7b00112.

[18] K. Nitu, P.L. Sanjaykumar, G.L. Jignasa, "Superior efficiency achievement for $FAPbI_3$-perovskite thin film solar cell by optimization with response surface methodology technique and partial replacement of Pb by Sn", *Optik*, vol. 176, pp. 262-277, 2019. doi: 10.1016/j.ijleo.2018.09.066.

[19] M. Saliba *et al.*, "Incorporation of rubidium cations into perovskite solar cells improves photovoltaic

performance", *Science*, vol. 354, no. 6309, pp. 206-209, 2016. doi: 10.1126/science.aah5557.

[20] J. M. Frost *et al.*, "Atomistic origins of high-performance in hybrid halide perovskite solar cells", *Nano Lett.*, vol. 14, no. 5, pp. 2584-2590, 2014. doi: 10.1021/nl500390f.

[21] W. Qiu *et al.*, "An interdiffusion method for highly performing cesium/formamidinium double cation perovskites", *Adv. Funct. Mater.*, vol. 27, no. 28, 1700920, 2017. doi: 10.1002/adfm.201700920.

[22] R. Yogamalar *et al.*, "X-ray peak broadening analysis in ZnO nanoparticles", *Solid State Commun*, vol. 149, pp. 1919-1923, 2009. doi: 10.1016/j.ssc.2009.07.043.

[23] G. K. Williamson and W. H. Hall, "X-ray line broadening from filed aluminium and wolfram," *Acta Metall.*, vol. 1, no. 1, pp. 22–31, 1953, doi: 10.1016/0001-6160(53)90006-6.

[24] A. Murphy, "Band-gap determination from diffuse reflectance measurements of semiconductor films, and application to photoelectrochemical water-splitting", *Sol. Energy Mater. Sol. Cells*, vol. 91, pp. 1326-1337, 2007. doi: 10.1016/j.solmat.2007.05.005.

[25] P. Kubelka and F. Munk, "Ein beitrag zur optik derFarbanstriche", *Zeitschrift fur Tech. Phys,* vol. 12, pp. 593-601, 1931.

[26]   B. Slimi *et al.*, "Perovskite $FA_{1-x}MA_xPbI_3$ for solar cells: film formation and properties", *Energy Procedia,* vol. 102, pp. 87-95, 2016. doi: 10.1016/j.egypro.2016.11.322.

[27] Y. Li, *et al.*, "Formamidinium-based lead halide perovskites: structure, properties, and fabrication methodologies", *Small Methods*, vol. 2, no. 7, 2018. doi: 10.1002/smtd.201700387.